

Development of a CMOS-Based Capacitive Tactile Sensor With Adjustable Sensing Range and Sensitivity Using Polymer Fill-In

Yu-Chia Liu, Chih-Ming Sun, Li-Yuan Lin, Ming-Han Tsai, and Weileun Fang

Abstract—This paper reports a capacitive-type CMOS-microelectromechanical system tactile sensor containing a capacitance-sensing gap filled with polymer. Thus, the equivalent stiffness of the tactile sensor can be modulated by the polymer fill-in, so as to further tune its sensing range. Moreover, the polymer fill-in has a higher dielectric constant to increase the sensitivity of the tactile sensor. In short, the sensing range and sensitivity of the proposed tactile sensor can be easily changed by using the polymer fill-in. In application, the tactile sensor and sensing circuits have been designed and implemented using the 1) TSMC 0.35 μm 2P4M CMOS process and the 2) in-house post-CMOS releasing and polymer-filling processes. The polydimethylsiloxane (PDMS) material with different curing agent ratios has been exploited as the fill-in polymers. The experiment results demonstrate that the equivalent stiffness of tactile sensors can be adjusted from 16.85 to 124.43 kN/m. Thus, the sensitivity of the tactile sensor increases from 1.5 to 42.7 mV/mN by varying the PDMS filling. Moreover, the maximum sensing load is also improved. [2009-0329]

Index Terms—CMOS MEMS, polymer fill-in, tactile sensor.

I. INTRODUCTION

THE STANDARD CMOS process is a mature approach to realize integrated circuits (ICs) and microelectronic components. It is easy to find the available foundry service to provide such fabrication processes. To date, the CMOS process has been employed to implement microelectromechanical systems (MEMS) devices. Such CMOS-MEMS technology attracts more attention in the area of microsensors since its capability of monolithic integration of mechanical components and ICs. In this regard, various MEMS sensors have been successfully developed using the standard CMOS fabrication platform. For instance, the MEMS sensing components includ-

ing mechanical, thermal, chemical, and biological sensors have been reported in [1]–[4].

The tactile sensor can act as a key component for the human-machine interface. Currently, the tactile sensor has found extensive applications in robot arm, medical instrument, consumer electronics (such as mobile phone, notebook), etc. Many MEMS tactile sensors, including the piezoresistive, piezoelectric, and capacitive-sensing devices, have been reported [5]–[8]. Typically, the performances of the piezoresistive-based tactile sensors are sensitive to the diffusion concentration and temperature variation [5]. Moreover, the piezoelectric-based tactile sensors are suffering from the poling field effect and the response problems [6]. The silicon-based process is considered as a promising approach for capacitive-type tactile sensors [7]. However, various issues, such as parasitic capacitance, cannot be ignored [8]. The CMOS-MEMS technology is also a potential approach to realize the capacitive-type tactile sensor [9], [10]. The main advantage of CMOS-MEMS technology is to enable the monolithic integration of mechanical structure and sensing circuits. Thus, the impedance mismatch and noise can be reduced [11]. However, the thickness and stiffness of the sensing membrane and the space between the sensing electrodes are limited by the standard film stacking of CMOS processes. Thus, the design and performance of the tactile sensor, such as the sensing range and the sensitivity, are also limited by the standard CMOS process. Moreover, the polymer material has been extensively employed to fabricate flexible tactile sensors [12]–[14].

The specifications of microtactile sensors, such as the sensing range and sensitivity, vary with different applications [15]. The design of the micromachined structure is employed to change the characteristics of microtactile sensors to meet the required specifications. For instance, the tactile sensor with stiff loading membrane can tolerate larger load and has wider sensing range. However, its sensitivity is reduced and could not be employed to detect small force. It would be useful to easily change the sensitivity and sensing range of the microtactile sensors for different applications. As limited to the standard CMOS processes, it is difficult to change the thickness of the loading membrane for the CMOS-MEMS tactile sensor. Thus, it is necessary to change the planar dimensions of the loading membrane and the photomasks for CMOS-MEMS tactile sensors of different specifications. This paper employs the polymer fill-in to adjust the sensitivity and sensing range of the CMOS-MEMS tactile sensor without changing the photomask.

Manuscript received December 25, 2009; revised August 22, 2010; accepted October 5, 2010. Date of publication December 6, 2010; date of current version February 2, 2011. This work was supported in part by the Ministry of Economic Affairs of Taiwan under Grant 98-EC-17-A-07-S2-0095 and in part by the National Science Council of Taiwan under Grant NSC-96-2628-E-007-008-MY3. Subject Editor Y. B. Gianchandani.

Y.-C. Liu, C.-M. Sun, and M.-H. Tsai are with the Institute of NanoEngineering and MicroSystems, National Tsing Hua University, Hsinchu 30013, Taiwan.

L.-Y. Lin is with the Power Mechanical Engineering Department, National Tsing Hua University, Hsinchu 30013, Taiwan.

W. Fang is with the Institute of NanoEngineering and MicroSystems, National Tsing Hua University, Hsinchu 30013, Taiwan, and also with the Power Mechanical Engineering Department, National Tsing Hua University, Hsinchu 30013, Taiwan (e-mail: fang@pme.nthu.edu.tw).

Color versions of one or more of the figures in this paper are available online at <http://ieeexplore.ieee.org>.

Digital Object Identifier 10.1109/JMEMS.2010.2090494

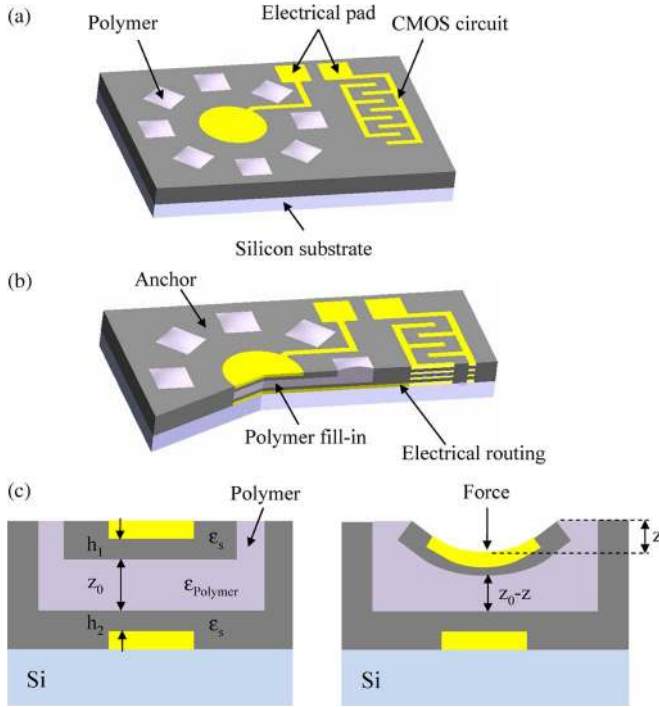


Fig. 1. (a) The schematic design of the proposed CMOS-MEMS tactile sensor with polymer fill-in, (b) the cross section view of the device, and (c) the load-deflection of tactile sensor with composite membrane and polymer fill-in.

The technique to combine the polymer process to change the characteristics of the microsensor has been reported in [16], [17]. The development of a CMOS-MEMS capacitive tactile sensor with adjustable sensing range, as well as sensitivity, using the polymer fill-in approach is proposed in [18]. This paper discussed the design and analysis of the CMOS-MEMS tactile sensor with polymer fill-in. In application, the capacitive tactile sensor is implemented using the Taiwan Semiconductor Manufacturing Company (TSMC) 0.35 μm 2-Polysilicon 4-Metal (2P4M) CMOS process and the in-house post-CMOS process. Moreover, the polydimethylsiloxane (PDMS) is employed to fill into the sensing gap of the tactile sensor, and the varying of the characteristics (sensitivity, sensing range, etc.) of tactile sensor is demonstrated by using the PDMS with different curing agent ratios. The mechanical and electrical characteristics of the polymer fill-in and their influences on the microtactile sensor are also investigated.

II. SENSOR DESIGN AND ANALYSIS

Fig. 1 shows the schematic illustration of the tactile sensor design. As shown in Fig. 1(a) and (b), the capacitive-type tactile sensor consists of the deformable loading membrane (formed by the dielectric and metal films of CMOS process), stationary sensing electrodes (formed by metal films of the CMOS process), and the polymer fill-in (formed by the post-CMOS process). The equivalent stiffness K_{eq} of the tactile sensor is contributed from not only the deformable loading membrane but also the polymer fill-in. The schematic illustrations in Fig. 1(c) show the sensor before and after applying a tactile force F on its loading membrane. The sensing electrodes have an initial gap of z_0 . As the loading membrane deformed

by force F , the gap between the sensing electrodes will be changed. Thus, the tactile force can be detected by the capacitance change between the sensing electrodes. As shown in Fig. 1(c), the loading membrane of the proposed CMOS-based tactile sensor is consisted of the metal-dielectric composite layers. As reported in [9], the initial sensing capacitance C_0 of such tactile sensor with air gap is expressed as

$$C_0 = \frac{\epsilon_0 A}{(h_1 + h_2) \frac{\epsilon_0}{\epsilon_s} + z_0} \quad (1)$$

where ϵ_0 is the permittivity of air; ϵ_s is the dielectric constant of silicon oxide; A is the overlap area of the sensing electrodes; and h_1 and h_2 are oxide thickness. After considering the gap with polymer fill-in, the initial sensing capacitance C_0 becomes

$$C_0 = \frac{\epsilon_{\text{Polymer}} A}{(h_1 + h_2) \frac{\epsilon_{\text{Polymer}}}{\epsilon_s} + z_0} \quad (2)$$

where $\epsilon_{\text{polymer}}$ is the dielectric constant of polymer fill-in. In short, the sensitivity and sensing range of the tactile sensor can be adjusted by varying the stiffness and the dielectric constant of polymer fill-in. Thus, the specifications of tactile sensor can be easily adjusted by the polymer filling process without modifying the design of the CMOS-MEMS components.

This paper employed the flexible and stable PDMS as the polymer fill-in to demonstrate the proposed concept. Thus, the stiffness and the dielectric constant of the PDMS can be changed by varying the ratio of its curing agent. Moreover, the PDMS has a very low drift of the mechanical properties [19], [20]. Three types of PDMS (*Sylgard 527*, Dow Corning Corporation), respectively with curing agent ratios of 1 : 1, 1 : 5, and 1 : 10 (named 1 : 1 PDMS, 1 : 5 PDMS, and 1 : 10 PDMS in the following text) have been exploited as the polymer fill-in. Fig. 2 shows the characterized electrical and mechanical properties of these three types of PDMS. Fig. 2(a) shows the dielectric constant measured using the LCR meter (E4980A, Agilent) within the modulation frequency from 50 Hz to 10 kHz. The average dielectric constants ϵ_{PDMS} of 1 : 1 PDMS, 1 : 5 PDMS, and 1 : 10 PDMS are 3, 2.89, and 2.86, respectively. Hence, the dielectric constant of PDMS ϵ_{PDMS} is much larger than that of air ϵ_0 . Moreover, the variation of dielectric property of the PDMS under a large deformation has been characterized. In this test, the 5-mm-thick PDMS samples were prepared and then deformed by external load. The dielectric constant of PDMS was characterized at different sample deformations. As indicated in Fig. 2(b), the variation of the PDMS dielectric constant is less than 4% even the sample has a large compressive strain of 60%. Thus, to simplify the analysis and simulation, this study considered the dielectric constant of PDMS as a constant. Furthermore, the elastic modules of different types PDMS were determined from the tensile test by using a commercial testing system (Instron 8848, Instron Corporation). As shown in Fig. 2(c), the measured elastic moduli of these three types PDMS were 29 kPa (1 : 1 PDMS), 672 kPa (1 : 5 PDMS), and 1120 kPa (1 : 10 PDMS), respectively. Moreover, the Poisson's ratios of these three types PDMS were also characterized as 0.495 (1 : 1 PDMS), 0.491 (1 : 5 PDMS), and 0.485 (1 : 10 PDMS), respectively. In comparison, the Poisson's

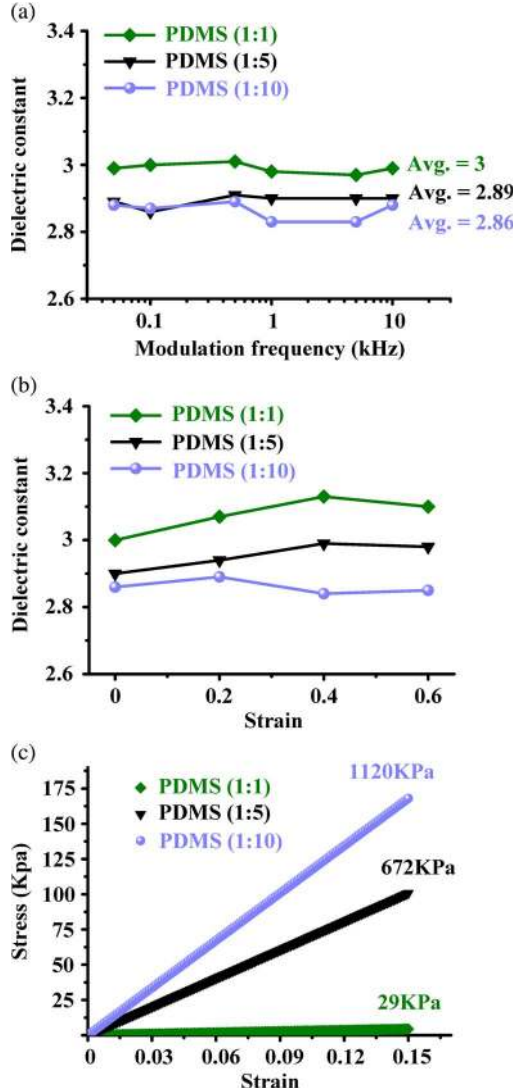


Fig. 2. Characteristics of the PDMS with different curing agent ratios, (a) the dielectric constants measured from the LCR meter, (b) the variation of dielectric constant at different strain conditions, and (c) the elastic modules determined from the microtensile testing.

ratio reported in [21] is 0.499. Thus, the equivalent stiffness of the tactile sensor can be adjusted by using different polymer fill-in so that the sensitivity and sensing range of the tactile sensor are easily changed.

Table I summarizes a typical sensor design and its initial sensing capacitance. The ideal initial sensing capacitances are respectively predicted from (1) and (2) and the commercial finite element software (CoventorWare). In this ideal case, the initial deformation of the loading membrane resulted from the thin film residual stresses and the shrinkage of polymer fill-in are not considered. The results show the initial sensing capacitance, as well as the sensitivity of the tactile sensor can be adjusted by the polymer fill-in. This paper also established the finite element model in Fig. 3(a) using CoventorWare to predict the performance of tactile sensors with different polymer fill-in. The simulation model consists of the loading membrane (partially anchored to the substrate) and the surrounded polymer fill-in. The elastic modulus of PDMS is determined from Fig. 2(c), and the measured Poisson's ratio of PDMS is also em-

TABLE I
PREDICTED AND MEASURED INITIAL SENSING CAPACITANCES AT DIFFERENT CONDITIONS

Design parameter	Gap material			
	Air	PDMS (1:1)	PDMS (1:5)	PDMS (1:10)
Dielectric constant	1	3	2.89	2.86
Sensing area, A (μm^2)	$\pi(110)^2$			
Sensing gap, z_0 (μm)	2.28			
Ideal case (No initial deformation of loading membrane)				
Initial sensing capacitance, C_0 (fF) (Eqs.(1)-(2))	120	264	258	257
Initial sensing capacitance, C_0 (fF) (CoventorWare)	121	259	254	252
Real case (With initial deformation of loading membrane)				
Initial sensing capacitance, C_0 (fF) (CoventorWare)	148	292	299	348
Initial sensing capacitance, C_0 (fF) (measured)	153 ± 4	300 ± 2	315 ± 5	363 ± 10

ployed in the model. The typical simulation result in Fig. 3(b) displays the deformation of the loading membrane after applying a prescribed deflection at its center. The simulation results in Fig. 3(c) further show the variation of the capacitance change with the central deformation of loading membrane for tactile sensors with different polymer fill-in. Since the 1:1 PDMS has a much smaller stiffness, for a given central deformation of loading membrane, the sensor with 1:1 PDMS fill-in has a larger capacitance change than those with 1:5 and 1:10 PDMS fill-in. Since the 1:1 PDMS has a larger dielectric constant, for a given central deformation of loading membrane, the sensor with 1:1 PDMS fill-in has a higher capacitance change than that with air gap. Note the equivalent stiffnesses of these four cases are different. In summary, the stiffness and the dielectric constant of the polymer fill-in can be employed to adjust the sensitivity of the proposed tactile sensor.

To detect the signal variation of the tactile sensor monolithically, a wide-swing and folded-cascode operation transconductance amplifier (OTA) is used as the sensing circuit [22]. Fig. 4(a) shows a wide-swing differential amplifier which extends the input common mode range (ICMR) by combining both the p- and n-channel MOS input differential pairs. Simulation results show that the OTA has a 70-dB open loop gain, 30-MHz unit gain bandwidth with around 80° phase margin at a 2-pF load, and its power consumption is only 1.2 mW. The sensing signal can be accurately detected by the designed close loop systems, as shown in Fig. 4(b).

III. POST-CMOS FABRICATION AND RESULTS

Fig. 5(a) shows the planar design of the fabricated device including a CMOS-MEMS tactile sensor and a fabrication test key. Some important dimensions of the device are listed in Table II. Fig. 5(b)–(g) show the process steps along the FF' cross section in Fig. 5(a) to implement the proposed devices, including the capacitive-type tactile sensor with polymer fill-in and the monolithic integrated sensing circuit. In addition, the

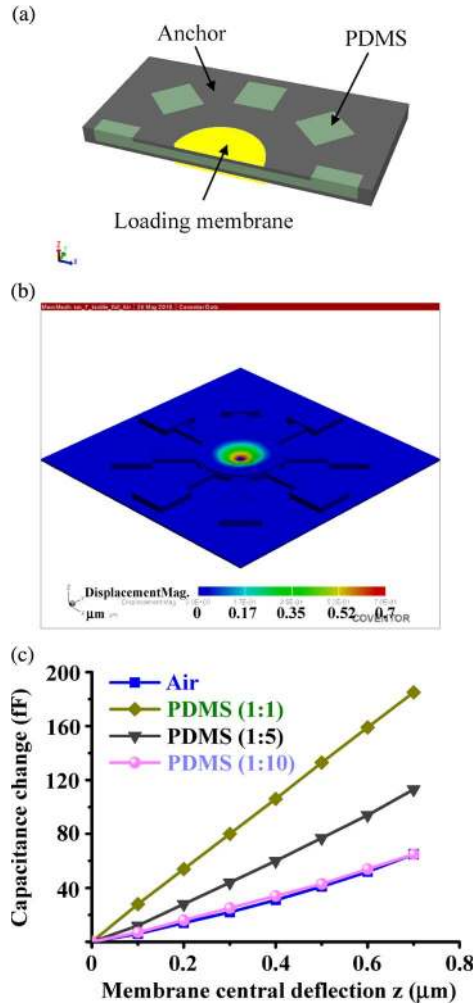


Fig. 3. Finite element model and simulation results, (a) the finite element model, (b) the deformation of loading membrane after applying a prescribed deflection at its center, and (c) the variation of capacitance change with the loading membrane deformation for tactile sensors with different polymer fill-in.

test key formed by the transparent dielectric layers is also designed and implemented to monitor the metal wet under-etching and the polymer fill-in process. The fabrication mainly consists of the CMOS processes, the post-CMOS metal layers etching process, and the polymer filling process. As shown in Fig. 5(b), the thin film stacking and patterning of the proposed devices was firstly prepared by the Taiwan Semiconductor Manufacturing Company using the standard $0.35 \mu\text{m}$ 2P4M CMOS process. Fig. 5(c)–(g) show the post-CMOS processes. As shown in Fig. 5(c) and (d), the solution containing H_2SO_4 and H_2O_2 (with mixing ratio $\text{H}_2\text{SO}_4 : \text{H}_2\text{O}_2 = 2 : 1$) was used to etch through the metal layers and tungsten vias [23], [24]. Dielectric layers acted as a protection film during the metal wet etching. In addition, the dielectric film distributed along the path of the metal wet etching was also employed as a protection layer in this process. As the surrounding metal layers are fully removed, the dielectric blocks were released from the substrate, as shown in Fig. 5(c). Following the same step in Fig. 5(c), the metal layers and dielectric blocks were removed until the etching solution reached the dielectric protection layer, as shown in Fig. 5(d). These etch release holes were acted as the polymer

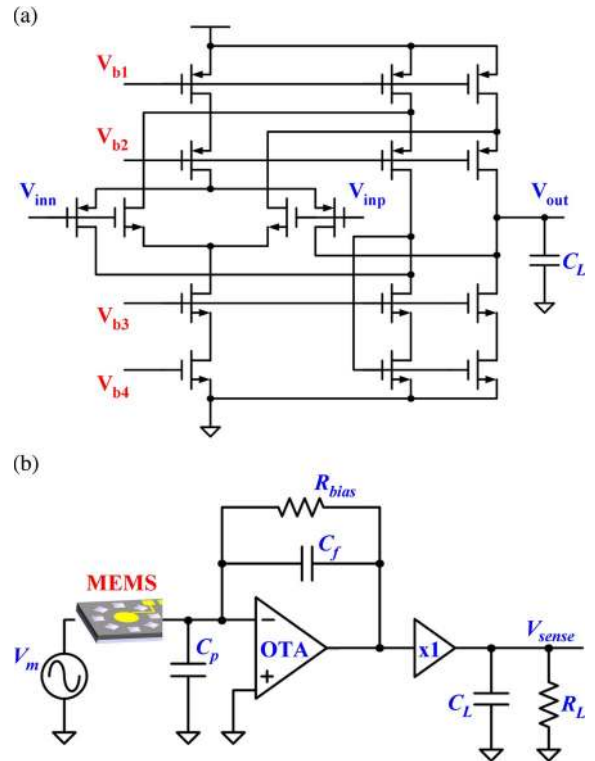


Fig. 4. (a) Schematic of wide-swing folded-cascode OTA, (b) architecture of mechanical and electrical parts combination.

injection and air exhaust holes in the following polymer fill-in process. The dielectric film was employed as the etching stop layer in this process. Moreover, this paper employed the metal 2 and 3 layers and the tungsten via between these two metal layers to define the sensing gap. Thus, the loading membrane was suspended with a sensing gap of $2.28 \mu\text{m}$. After that, the polymer was filled into the etch release holes and sensing gap, as shown in Fig. 5(e). The selected PDMS polymer (*Sylgard 527*) has a smaller viscosity of 425 cP. As shown in Fig. 5(e), the PDMS was dispensed on the substrate by the commercial pneumatic dispensing workstation (EFD 2400, EFD Inc.). The volume of dispensed PDMS was controlled by the dispensing time and pressure of the workstation. After that, the PDMS was pulled into the gap under the loading membrane through the channel by means of the capillary force [25]. Meanwhile, the air inside the sensing gap was released from the air exhaust holes. The test key consisted of the transparent dielectric film was exploited to monitor the polymer filling process. As shown in Fig. 5(f), the substrate was then placed into the vacuum chamber to ensure the sensing gap fully filled with PDMS. After that, the PDMS was cured in room temperature. Finally, reactive ion etching was used to remove residual polymer and passivation layer for wire bonding, as shown in Fig. 5(g). Fig. 6 shows typical fabrication results. The optical images in Fig. 6(a) and (b) show the test key during metal wet etching processes. The residual metal layer under the transparent test key is clearly shown in Fig. 6(a). The metal layer under the transparent test key is fully in Fig. 6(b). The SEM micrographs in Fig. 6(c) and (d) show the released loading membrane before the filling of PDMS, and the etching release hole (also acted as the polymer inlet hole) are also clearly observed.

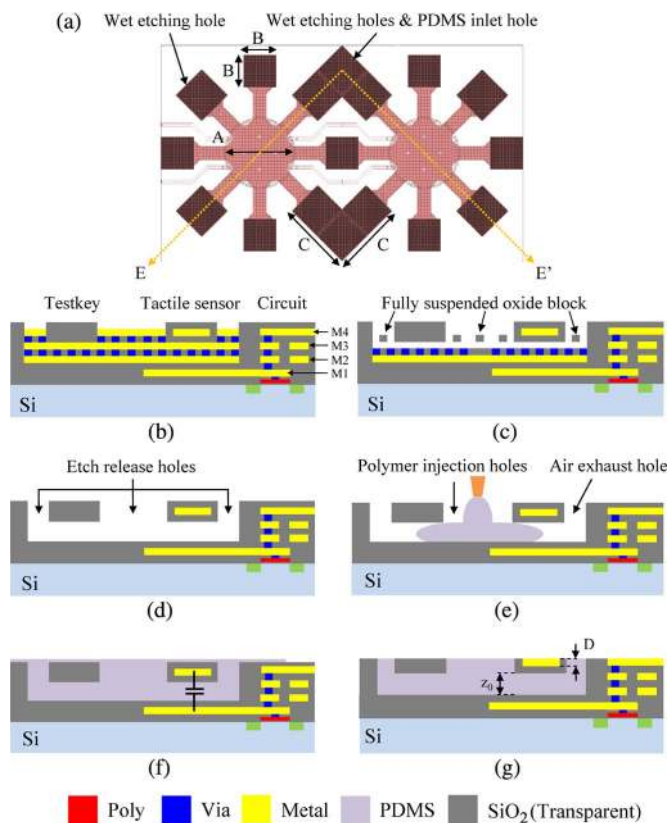


Fig. 5. (a) The planar design of the fabricated device and test key, (b) the chip prepared by the standard TSMC 2P4M CMOS process, and (c)–(g) the in-house post-CMOS releasing and polymer fill-in processes.

TABLE II
DESIGN PARAMETERS OF A TYPICAL TACTILE SENSOR

Geometry of sensing unit	Dimension
Sensing membrane, A (μm)	220
Etching hole, B (μm)	100
Etching & PDMS inlet hole, C (μm)	200
Top electrode thickness, D (μm)	1.93
Initial sensing gap, z_0 (μm)	2.28

As discussed in Section II, three types of PDMS with curing agent ratios of 1 : 1, 1 : 5, and 1 : 10 were respectively employed as the fill-in polymer. The photographs in Fig. 7 respectively show the tactile sensors during the filling of PDMS. The tactile sensor with a metal electrode is located in the left-hand side of the photograph. The test key consisting of the transparent membrane is located in the right-hand side of the photograph and is employed to monitor the polymer filling status. The PDMS was firstly dispensed on the inlet hole, as shown in Fig. 7(a). The polymer was gradually diffused into the sensing gap, and the air was released from the exhaust holes. Moreover, as observed from the test key in Fig. 7(a), the gap underneath the transparent dielectric films was partially filled with the PDMS which corresponds to the process shown in Fig. 5(e). The photograph in Fig. 7(b) shows the PDMS was fully filled the sensing gap underneath the loading membrane of the test key and the tactile sensor and also came out from all of

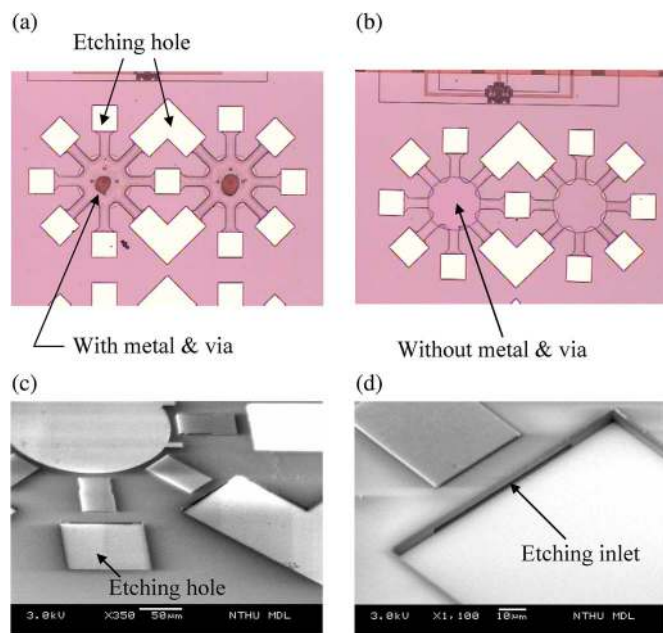


Fig. 6. (a) and (b) The transparent test key observed under the optical microscope and (c) and (d) the SEM micrographs of tactile sensors, and the etching holes and channels are observed.

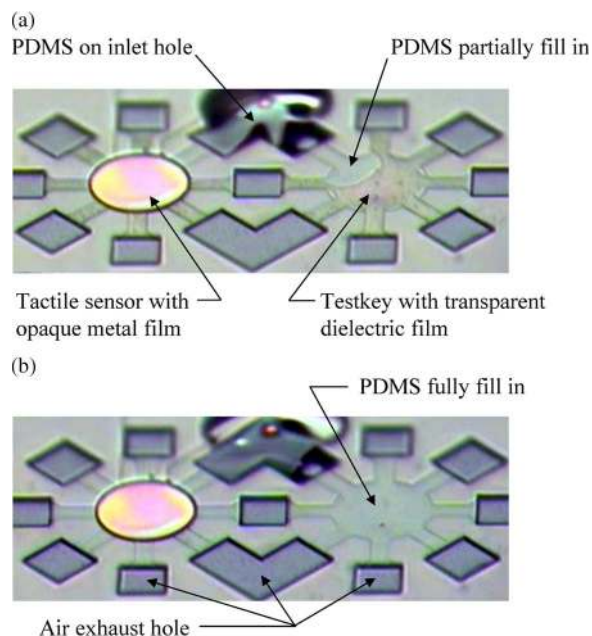


Fig. 7. Polymer fill-in processes monitored through the transparent test key, (a) partially fill with PDMS under sensing gap, and (b) fully filled with PDMS under sensing gap.

the exhaust holes. This condition corresponds to the process step shown in Fig. 5(f). It demonstrates the sensing gap was successfully filled with polymer using the proposed approach.

IV. EXPERIMENT RESULTS AND DISCUSSION

This paper employed various approaches to characterize and test the fabricated tactile sensors. First, the initial shape of the loading membrane was characterized using the optical interferometer. The measurement results in Fig. 8(a) respectively show the typical surface topographies of the loading membrane with

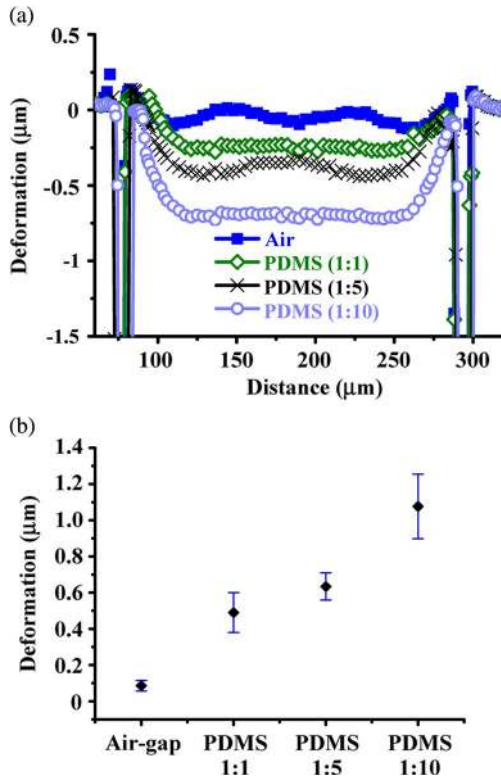


Fig. 8. (a) The measured surface profile of the suspended sensing membranes with different PDMS fill-in and (b) the measured initial deformation of loading membrane for different PDMS fill-in (average from five samples for each case).

different polymer fill-in. The diameter of the loading membrane is $220 \mu\text{m}$. Fig. 8(b) shows the average initial deformation of the tactile sensors (average from five samples for each case) with different PDMS fill-in. The measurement results for air gap indicate the loading membrane has a small initial downward deformation of near $0.09 \pm 0.03 \mu\text{m}$ caused by the residual stresses of thin films. However, due to the shrinkage of the polymer after curing, the loading membrane of the tactile sensors with PDMS fill-in has larger initial deformation. According to measurements, the loading membranes with different PDMS fill-in are bent downward with initial deformations of $0.49 \pm 0.11 \mu\text{m}$ (for 1 : 1 PDMS), $0.63 \pm 0.08 \mu\text{m}$ (for 1 : 5 PDMS), and $1.08 \pm 0.18 \mu\text{m}$ (for 1 : 10 PDMS), respectively. Moreover, the measured initial sensing capacitances were $153 \pm 4 \text{ fF}$ (air gap), $300 \pm 2 \text{ fF}$ (for 1 : 1 PDMS), $315 \pm 5 \text{ fF}$ (for 1 : 5 PDMS), and $363 \pm 10 \text{ fF}$ (for 1 : 10 PDMS), respectively. As indicated in Table I, after considering the initial deformation of the loading membrane, the initial sensing capacitances predicted by the CoventorWare software agree well with the measurements. In addition, the equivalent stiffness of tactile sensors was characterized by a commercial nanoindentation system. The loading membrane and the polymer fill-in were deformed by a probe during the test. The equivalent stiffness of loading membranes determined from the linear load-deflection curve are respectively 4.44 kN/m (with air gap), 16.85 kN/m (with 1 : 1 PDMS fill-in), 90.16 kN/m (with 1 : 5 PDMS fill-in), and 124.43 kN/m (with 1 : 10 PDMS fill-in). The measurement results demonstrate the equivalent stiffness of loading membrane can be easily tuned by changing the polymer filling-in.

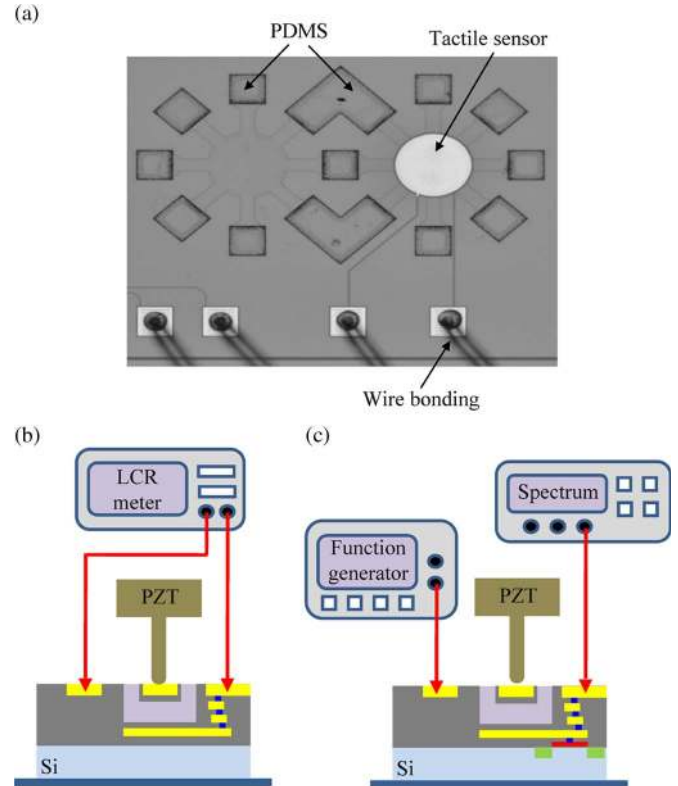


Fig. 9. (a) The tactile sensor chip after wire bonding and (b) and (c) the test setups to calibrate the capacitance change and output voltage of the tactile sensors at different loadings.

The chip after wire bonding was then packaged inside a ceramic case, as shown in Fig. 9(a). The experimental setup was established to characterize the variation of capacitance changes (ΔC) and output voltages (V) with the displacements. As shown in Fig. 9(b), a rigid probe was employed to apply a displacement at the center of loading membrane, and then the capacitance change resulted from the deformed membrane was measured by the LCR meter. The probe displacement was precisely controlled by the piezoelectric actuator with a resolution of 10 nm . The results in Fig. 10(a) respectively show the capacitance change from tactile sensors of different polymer fill-in as the central displacement of loading membrane ranging from 0 to $0.7 \mu\text{m}$. The membrane of tactile sensor with air gap was broken as its central deformation reached $0.7 \mu\text{m}$. The capacitance changes measured from the sensors with polymer fill-in increase linearly with the central displacements of loading membrane as the displacement smaller than $0.4 \mu\text{m}$ (for the 1 : 1 PDMS fill-in) or $0.5 \mu\text{m}$ (for the 1 : 5 and 1 : 10 PDMS fill-in). For a given central deformation of loading membrane, the sensor with 1 : 1 PDMS fill-in has a larger capacitance change than those with 1 : 5 and 1 : 10 PDMS fill-in. This result agrees well with the discussion in Section II that the stiffness of 1 : 1 PDMS is much smaller than those of 1 : 5 and 1 : 10 PDMS. In addition, for a given central deformation of loading membrane, the sensor with 1 : 1 PDMS fill-in has a much larger capacitance change than that with air-gap. This is mainly contributed by the higher dielectric constant of PDMS fill-in. Thus, the sensitivity change of tactile sensors using different polymer fill-in is demonstrated. As a result, the linear variation of capacitance change with the

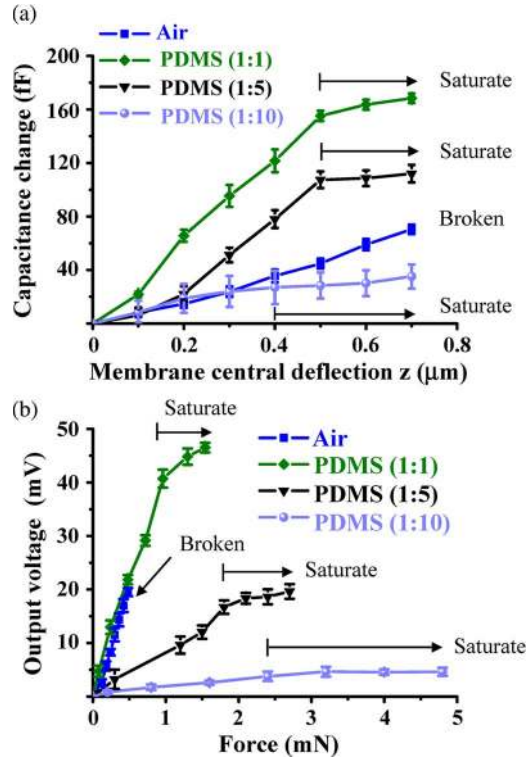


Fig. 10. Measurement results with respect to different tactile sensors, (a) the capacitance change versus the central displacement of loading membrane, and (b) the output voltage versus the applying load.

membrane deformation in Fig. 10(a) reasonably agrees with that in Fig. 3(c), although the measured capacitance change for sensors with 1:5 and 1:1 PDMS fill-in are higher than the simulation ones. Moreover, the capacitance change of sensors with polymer fill-in is significantly decreased (saturate) as the central displacement of loading membrane exceeds $0.4 \mu\text{m} \sim 0.5 \mu\text{m}$. It indicates that the central deformation of the membrane gradually reaches its limit due to the existence of PDMS. The test setup in Fig. 9(c) was also established to measure the output voltage detected from the monolithically integrated IC of the tactile sensor caused by the deformation of loading membrane. In addition, the equivalent stiffness of the loading membranes with or without polymer fill-in has been characterized by the nanoindentation system. Thus, the output voltage signals of the tactile sensors at different applying loads are determined, as shown in Fig. 10(b). Similar to Fig. 10(a), the measurement results also show a linear sensing range and a saturation range. Thus, the linearity as well as sensitivity of these tactile sensors is determined. Table III summarizes the typical measured performances of these tactile sensors. The measurement results also show that the loading membrane with air gap was broken as the applying force exceeded 0.5 mN . On the other hand, the output voltage of tactile sensors with PDMS-gap was saturated when the loading membrane was overloaded. It shows the PDMS fill-in can also act as a protection layer to prevent the loading membrane from damaging during the overload condition. Table IV shows the comparison of the sensitivity and sensing range of various tactile sensors.

TABLE III
CHARACTERIZATIONS OF THE TACTILE SENSORS WITH AIR GAP
DIFFERENT PDMS FILL-IN

Gap material	Air	PDMS (1:1)	PDMS (1:5)	PDMS (1:10)
Initial capacitance, C_0 (fF)	153 \pm 4	300 \pm 2	315 \pm 5	363 \pm 10
Young's modules (kPa)	NA	29	672	1120
Poisson's ratio	NA	0.495	0.491	0.485
Equivalent stiffness of loading membrane, K_{eq} (kN/m)	4.44	16.85	90.16	124.43
Sensitivity (mV/mN)	38.9	42.7	8.1	1.5
Sensing range (mN)	0~0.5	0~1	0~1.8	0~2.4
Non-linearity (%)	1.6	2.4	6.8	2.0

TABLE IV
COMPARISON OF THE SENSITIVITY AND SENSING RANGE
OF VARIOUS TACTILE SENSORS

	T. Salo [4]	A. Wisitorsaat [5]	K. Chun [7]	Z. Chu [8]
Process	CMOS-based	Metal on glass	Si-based	Si-based
Sensing mechanism	Capacitive	Piezoresistive	Capacitive	Capacitive
Sensor dimension	130 x 130 μm^2	200 x 200 μm^2	600 x 600 μm^2	900 x 900 μm^2
Sensitivity	9.8mV/mN	9.8mV/ μN	6.1mV/mN	13.3fF/mN
Full force loading	0~60mN	0~0.2mN	0~0.2N	0~9.8mN
	C.-T. Ko [9]	C.-C. Wen [17]	M. Adam [18]	This study
Process	CMOS-based	SOI-based	CMOS-based	CMOS-based
Sensing mechanism	Capacitive	Piezoresistive	Piezoresistive	Capacitive
Sensor dimension	75 x 75 μm^2	3 x 3 mm^2	300 x 300 μm^2	110 x 110 μm^2
Sensitivity	27.1kHz/ μN	0.52~3.36%/N	27.8mV/mN	1.5~42.7mV/mN
Full force loading	0~0.5mN	0~0.2N	0~1.8mN	0~2.4mN

V. CONCLUSION

In this paper, a capacitive type CMOS-MEMS tactile sensor containing a sensing gap filled with polymer has been proposed. The capacitive tactile sensor is implemented using the TSMC 0.35 μm 2P4M CMOS standard process and the in-house post-CMOS process. In addition, the flexible and stable PDMS is employed to fill into the sensing gap of the tactile sensor. Thus, the dielectric constant of the capacitance sensing gap and the equivalent stiffness of the loading membrane can be changed by the PDMS fill-in, so as to modulate the characteristics of the tactile sensor. Moreover, the characteristics of the polymer fill-in are easily tuned by changing the ratio of PDMS and its curing agent during the post-CMOS process. In other words, the sensing range and sensitivity of the proposed tactile sensor can be easily tuned by varying the characteristics of polymer fill-in. In applications, the PDMS of three different curing agent ratios have been employed as the polymer fill-in for the fabricated

CMOS-MEMS tactile sensors. The experiment results show that equivalent stiffness of tactile sensors can be tuned from 16.85 to 124.43 kN/m, and the sensitivity of the tactile sensor increases from 1.5 to 42.7 mV/mN by varying the PDMS fill-in. The polymer fill-in also acts as the protection layer to prevent the broken of loading membrane during the overload condition. Nevertheless, the viscoelastic property of polymer fill-in is a critical consideration for the proposed design.

ACKNOWLEDGMENT

The authors would like to thank the TSMC and the National Chip Implementation Center, Taiwan, for the support of CMOS chip manufacturing. The authors would also like to thank National Tsing Hua University and National Chiao Tung University for providing the fabrication facilities.

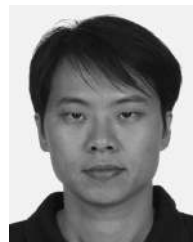
REFERENCES

- [1] J. Verd, A. Uranga, G. Abadal, J. Teva, F. Torres, J. L. Lopez, F. Perez-Murano, J. Esteve, and N. Barniol, "Monolithic CMOS MEMS oscillator circuit for sensing in the attogram range," *IEEE Electron Device Lett.*, vol. 29, no. 2, pp. 146–148, Feb. 2008.
- [2] S. Eminoglu, D. S. Tezcan, M. Y. Tanrikulu, and T. Akin, "Low-cost uncooled infrared detectors in CMOS process," *Sens. Actuator A, Phys.*, vol. 109, no. 1/2, pp. 102–113, Dec. 2003.
- [3] C. Hagleitner, D. Lange, A. Hierlemann, O. Brand, and H. Baltes, "CMOS single-chip gas detection system comprising capacitive calorimetric, and mass-sensitive sensors," *IEEE J. Solid-State Circuits*, vol. 37, no. 12, pp. 1867–1878, Dec. 2002.
- [4] T. Salo, K.-U. Kirstein, T. Vancura, and H. Baltes, "CMOS-based tactile microsensor for medical instrumentation," *IEEE Sensors J.*, vol. 7, no. 2, pp. 258–265, Feb. 2007.
- [5] A. Wisitoraat, V. Patthanasetakul, T. Lomas, and A. Tuantranont, "Low cost thin film based piezoresistive MEMS tactile sensor," *Sens. Actuator A, Phys.*, vol. 139, no. 1/2, pp. 17–22, Sep. 2007.
- [6] C. Li, P.-M. Wu, S. Lee, A. Gorton, M. J. Schulz, and C. H. Ahn, "Flexible dome and bump shape piezoelectric tactile sensors using PVDF-TrFE copolymer," *J. Microelectromech. Syst.*, vol. 17, no. 2, pp. 334–341, Apr. 2008.
- [7] K. J. Chun and K. D. Wise, "A high-performance silicon tactile imaging based on a capacitive cell," *IEEE Trans. Electron Devices*, vol. ED-32, no. 7, pp. 1196–1201, Jul. 1985.
- [8] Z. Chu, P. M. Sarro, and S. Middelhoek, "Silicon three-axial tactile sensor," *Sens. Actuator A, Phys.*, vol. 54, no. 1–3, pp. 505–510, Jun. 1996.
- [9] C.-T. Ko, S.-H. Tseng, and M. S.-C. Lu, "A CMOS micromachined capacitive tactile sensor with high-frequency output," *J. Microelectromech. Syst.*, vol. 15, no. 6, pp. 1708–1714, Dec. 2006.
- [10] N. Sato, S. Shigematsu, H. Morimura, M. Yano, K. Kudou, T. Kamei, and K. Machida, "Novel surface structure and its fabrication process for MEMS fingerprint sensor," *IEEE Trans. Electron Devices*, vol. 52, no. 5, pp. 1026–1032, May 2005.
- [11] H. Baltes, O. Brand, A. Hierlemann, D. Lange, and C. Hagleitner, "CMOS MEMS—Present and future," in *Proc. IEEE Int. Conf. Micro Electro Mech. Syst.*, Las Vegas, NV, Jan. 2002, pp. 459–466.
- [12] J. Engel, J. Chen, and C. Liu, "Development of polyimide flexible tactile sensor skin," *J. Micromech. Microeng.*, vol. 13, no. 3, pp. 359–366, Feb. 2003.
- [13] H. K. Lee, S. I. Chang, and E. Yoon, "A flexible polymer tactile sensor: Fabrication and modular expandability for large area deployment," *J. Microelectromech. Syst.*, vol. 15, no. 6, pp. 1681–1685, Dec. 2006.
- [14] M.-Y. Cheng, X.-H. Huang, C.-W. Ma, and Y.-J. Yang, "A flexible capacitive tactile sensing array with floating electrodes," *J. Micromech. Microeng.*, vol. 19, no. 11, p. 115 001, Sep. 2009.
- [15] E. Pritchard, M. Mahfouz, B. Evans, III, S. Eliza, and M. Haider, "Flexible capacitive sensors for high resolution pressure measurement," in *Proc. IEEE Int. Conf. Sensors*, Lecce, Italy, Oct. 2008, pp. 1484–1487.
- [16] Y.-C. Liu, C.-M. Sun, L.-Y. Lin, M.-H. Tsai, and W. Fang, "A tunable range/sensitivity CMOS-MEMS capacitive tactile sensor with polymer fill-in technique," in *Proc. IEEE Int. Conf. Transducers*, Denver, CO, Jun. 2009, pp. 2190–2193.
- [17] C.-C. Wen and W. Fang, "Tuning the sensing range and sensitivity of three axes tactile sensors using the polymer composite membrane," *Sens. Actuator A, Phys.*, vol. 145/146, pp. 14–22, Jul./Aug. 2008.
- [18] M. Adam, T. Mohacsy, P. Jonas, C. Ducso, E. Vazsonyi, and I. Barsony, "CMOS integrated tactile sensor array by porous Si bulk micromachining," *Sens. Actuator A, Phys.*, vol. 142, no. 1, pp. 192–195, Mar. 2008.
- [19] J. C. Lotters, W. Olthuis, P. H. Veltink, and P. Bergveld, "Polydimethylsiloxane as an elastic material applied in a capacitive accelerometer," *J. Micromech. Microeng.*, vol. 6, no. 1, pp. 52–54, Mar. 1996.
- [20] J. C. Lotters, W. Olthuis, P. H. Veltink, and P. Bergveld, "The mechanical properties of the rubber elastic polymer polydimethylsiloxane for sensor application," *J. Micromech. Microeng.*, vol. 7, no. 3, pp. 145–147, Sep. 1997.
- [21] P. Peng, R. Rajamani, and A. G. Erdman, "Flexible tactile sensor for tissue elasticity measurement," *J. Microelectromech. Syst.*, vol. 18, no. 6, pp. 1226–1233, Dec. 2009.
- [22] F. Roewer and U. Kleine, "A novel class of complementary folded-cascade opamps for low voltage," *IEEE J. Solid-State Circuits*, vol. 37, no. 8, pp. 1080–1083, Aug. 2002.
- [23] C. Wang, M.-H. Tsai, C.-M. Sun, and W. Fang, "A novel CMOS out-of-plane accelerometer with fully differential gap-closing capacitance sensing electrodes," *J. Micromech. Microeng.*, vol. 17, no. 7, pp. 1275–1280, Jun. 2007.
- [24] M.-H. Tsai, C.-M. Sun, Y.-C. Liu, C. Wang, and W. Fang, "Design and fabrication of a metal wet-etching post-process for the improvement of CMOS-MEMS capacitive sensors," *J. Micromech. Microeng.*, vol. 19, no. 10, p. 105 017, Sep. 2009.
- [25] N. Lazarus, S. S. Bedair, C.-C. Lo, and G. K. Fedder, "CMOS-MEMS capacitive humidity sensor," *J. Microelectromech. Syst.*, vol. 19, no. 1, pp. 183–191, Feb. 2010.



Yu-Chia Liu was born in Kaohsiung, Taiwan, in 1985. He received the Master's degree in 2009 from the Institute of NanoEngineering and MicroSystems, National Tsing Hua University, Hsinchu, Taiwan, where he is currently working toward the Ph.D. degree.

His major research interests include CMOS MEMS capacitive sensing interface, CMOS MEMS sensors, and readout circuit design.



Chih-Ming Sun was born in Taipei, Taiwan, in 1981. He received the Ph.D. degree from the Institute of NanoEngineering and MicroSystems, National Tsing Hua University, Hsinchu, Taiwan, in 2010.

From April 2009 to January 2010, he was with Prof. G. K. Fedder at Carnegie Mellon University as a Visiting Student. His major research interests include CMOS-MEMS capacitive inertial sensors, CMOS-MEMS post processing, and sensors integration.



Li-Yuan Lin was born in Pingtung, Taiwan, in 1985. He received the Master's degree from the Power Mechanical Engineering Department, National Tsing Hua University, Hsinchu, Taiwan, in 2009.

His major research interests include piezoresistive sensors and flexible tactile sensor design.



Ming-Han Tsai was born in Yunlin, Taiwan, in 1982. He received the Master's degree in 2007 from the Institute of NanoEngineering and MicroSystems, National Tsing Hua University, Hsinchu, Taiwan, where he is currently working toward the Ph.D. degree.

His major research interests include CMOS-MEMS sensors and actuators and CMOS-MEMS post processing.



Weileun Fang was born in Taipei, Taiwan. He received the Ph.D. degree from Carnegie Mellon University, Pittsburgh, PA, in 1995. His doctoral research focused on the determination of the mechanical properties of thin films using micromachined structures.

In 1995, he was a Postdoctoral Researcher at Synchrotron Radiation Research Center, Taiwan. He joined the Power Mechanical Engineering Department, National Tsing Hua University, Hsinchu, Taiwan, in 1996, where he is currently a Professor as well as a faculty member of the NEMS Institute. In 1999, he was with Prof. Y.-C. Tai at California Institute of Technology as a Visiting Associate. His research interests include MEMS, with emphasis on micro fabrication/packaging technologies, CMOS MEMS, CNT MEMS, micro optical systems, micro sensors and actuators, and characterization of thin film mechanical properties. He also serves as a technical consultant for many MEMS companies in Taiwan.

Prof. Fang is currently a Board Member of JMM, and an Associate Editor of JM3. He has served as the Chief Delegate of Taiwan to the World Micro-machine Summit since 2008. He also served as the TPC of IEEE MEMS'04, MEMS'07, and MEMS'10, the regional TPC of Transducers'07, and the EPC of Transducers'09. He has been a member of the International Steering Committee of Transducers since 2009.